Appl. Phys. B 85, 223–229 (2006)
DOI: 10.1007/s00340-006-2343-6

Applied Physics B
Lasers and Optics

S. BORRI[1,2]
S. BARTALINI[2,3,✉]
P. DE NATALE[2,3]
M. INGUSCIO[1,2]
C. GMACHL[4]
F. CAPASSO[5]
D.L. SIVCO[6]
A.Y. CHO[6]

Frequency modulation spectroscopy by means of quantum-cascade lasers

[1] Dipartimento di Fisica dell'Università di Firenze, Via G. Sansone 1, 50019 Sesto Fiorentino (FI), Italy
[2] European Laboratory for Non–Linear Spectroscopy (LENS), Via N. Carrara 1, 50019 Sesto Fiorentino (FI), Italy
[3] CNR – Istituto Nazionale di Ottica Applicata (INOA), Largo E. Fermi 6, 50125 Firenze, Italy
[4] Electrical Engineering Dept., Princeton University, Princeton, NJ 08544, USA
[5] Division of Engineering and Applied Sciences, Harvard University, Cambridge, MA 02138, USA
[6] Bell Laboratories, Lucent Technologies, 600 Mountain Ave., Murray Hill, NJ 07974, USA

Received: 5 April 2006/Revised version: 19 May 2006
Published online: 7 July 2006 •

ABSTRACT In this paper we investigate the performance of quantum cascade (QC) lasers for high frequency modulation spectroscopy, particularly using frequency modulation (FM) and two-tone (2T) techniques. The coupling of the rf signal to the QC laser through the cryostat is studied in detail as well as the noise contributions of both the detector and the laser source to the final spectra. The experimental traces are obtained by spectroscopy on low-pressure N_2O and CH_4 gases at 8.0 μm and 7.3 μm wavelength, respectively, and reproduce the line profiles predicted by theory. As a preliminary result, an enhancement of a factor six is measured with respect to direct absorption line recording.

PACS 42.62.Fi; 42.72.A1; 07.88.+y

1 Introduction

Right after the first successful applications of frequency modulation techniques to optical heterodyne spectroscopy with standard laser set-ups (for example dye lasers [1]), it was clear that the more recent diode lasers would have been particularly well suited for these techniques. In fact they permit a direct modulation of the optical radiation by means of the supply current, so that additional devices, such as electro–optic modulators, are no longer needed.

Moreover, laser diodes presently cover most of the near-infrared spectral region, up to 2 μm, thus allowing high-precision spectroscopy on a wide range of molecular transitions with moderate sensitivity. Quantum-cascade (QC) lasers finally extend the peculiar features of laser diodes at longer wavelengths.

Since their birth, in 1994 [2], QC lasers have shown tremendous performance improvements and technological progress. At present, they are the only semiconductor lasers operating at room temperature [3–5] in the 4–24 μm wavelength range [6], in pulsed and continuous mode, with output power from tens of mW to several Watts [7]. These new devices are based on one type of carrier (electrons) jumping between energy levels created by quantum confinement [8]. The availability of high optical power, in addition to their high stability and monochromaticity, makes these devices very well fit for high sensitivity spectroscopy in the mid-infrared (MIR) spectral range. This region, in fact, represents a first choice for high sensitivity detection of many simple molecules, since their fundamental ro-vibrational transitions lay there. Even organic compounds exhibit strong absorption of light at MIR frequencies: medicine, process control, environmental science and many other scientific and technological branches have a strong demand for sensing systems. In the last decade QC lasers have been successfully used for mid-infrared spectroscopy [9, 10] and many scientists have improved QCLs performance and found new applications. QCLs linewidth reduction was demonstrated by frequency locking to resonant cavities [11, 12] and, very recently, adopting an extended-cavity configuration [13], whereas two groups have reported saturated absorption recording of Doppler lines [14, 15]. However, some questions, like the applicability of high-frequency modulation spectroscopic techniques to QC lasers, remain still open. Such techniques are well assessed techniques for high sensitivity spectroscopy with more "conventional" laser sources (for a review see, for example, Hall in [16]).

In this paper we report some experimental results obtained by implementing several frequency modulation techniques on QC lasers to detect molecular absorption lines. Advantages with respect to direct absorption and difficulties peculiar to QCLs are discussed.

2 Frequency-modulation techniques

In the following section, we will briefly recall the main theoretical points underlying the two techniques that we are testing on QC lasers: frequency modulation (FM) and two-tone (2T) spectroscopy.

2.1 *FM spectroscopy*

Frequency-modulation spectroscopy has long been implemented on diode lasers [17, 18] while its application to QC lasers represents a novelty. As described for the first time in [19], a high-frequency sinusoidal signal at a frequency $\nu_m = \omega_m/2\pi$ is added to the laser carrier (frequency $\nu_o = \omega_o/2\pi$ and amplitude E_0). The resulting signal becomes

✉ Fax: +39-055-4572451, E-mail:bartalini@lens.unifi.it

$$E(t) = \frac{1}{2} E_0 e^{i\omega_o t} \sum_{n=-\infty}^{+\infty} J_n(\beta) e^{in\omega_m t} + \text{c.c.}\,, \tag{1}$$

where $J_n(\beta)$ is the Bessel function of order n and β the modulation index. This signal is then composed by a carrier frequency with sidebands equally spaced (by the modulation frequency) whose amplitude depends on J_n. The signal then passes through a sample of length L with an absorption coefficient α and an index of refraction η. By defining the amplitude attenuation $\delta_j = \alpha_j L/2$ and the optical phase shift $\varphi_j = \eta_j L(\omega_o + j\omega_m)/c$ for the j-th signal sideband, the beat signal detected after the cell containing the substance under test can be written as

$$I(t) = \frac{cE_0^2}{8\pi} e^{-2\delta_0} \left[1 + (\delta_{-1} - \delta_1)\beta \cos\omega_m t - 2\left(\varphi_0 - \frac{\varphi_1 + \varphi_{-1}}{2}\right)\beta \sin\omega_m t \right], \tag{2}$$

where several approximations have been done (we have assumed that all the quantities β, $|\delta_0 - \delta_1|$, $|\delta_0 - \delta_{-1}|$, $|\varphi_0 - \varphi_1|$, $|\varphi_0 - \varphi_{-1}|$ are small compared with 1) [20]. We see that only the beating signal between the carrier and the two sidebands survives. This signal is composed of a dc and a sinusoidal component at a frequency ω_m. The in-phase ($\cos\omega_m t$) component of the beat signal is proportional to the difference in loss experienced by the upper and lower sidebands, whereas the quadrature component is proportional to the difference between the phase shift experienced by the carrier and the average of the phase shifts experienced by the sidebands. The beating signal is then demodulated by a mixer at the modulation frequency ω_m (and the detection phase adjusted in order to select one of the two contributions). The null signal that results with pure frequency-modulated light is due to a perfect cancellation of the rf signal arising from the upper sideband beating with the carrier with the rf signal from the lower sideband beating with the carrier. The high sensitivity to the phase or amplitude changes experienced by one of the sidebands results from the unbalance of this perfect cancellation.

The FM condition is achieved when ω_m is large compared with the spectral feature of interest and only one sideband at a time probes the spectral feature. In our experiment ω_m must be larger than the Doppler broadened N_2O line, Γ_D, at about 8.0 μm wavelength and room temperature ($\Gamma_D \simeq 120$ MHz FWHM).

The main advantage of this technique consists in the reduction of both the source and the detector noise in the acquired signal. In fact relevant information is shifted to radio-frequencies, where low-frequency noise is suppressed.

2.2 *Two-tone spectroscopy*

An important limitation of standard FM techniques essentially arises from the fact that, in the presence of pressure broadened lines (for example in atmospheric gas detection, where the linewidths can be as large as 10 GHz), high modulation frequencies are required and consequently detection/processing electronics must have huge bandwidths. The problem is even more important in the MIR region, where fast and sensitive detectors are really expensive, fragile and hard to be found even if we consider Doppler broadened lines.

The two-tone technique combines the advantages of standard FM with the benefits of a drastic reduction in detection bandwidth, with an additional improvement in signal-to-noise (S/N) ratio [21–23]. This technique was first proposed in 1982 for a tunable diode laser and small modulation frequencies (in the kHz range) [23] and then extended in 1986 to much higher frequencies (up to 16 GHz) [24] using a cw dye laser source and an electro–optic modulator. In the same year, high-frequency (hundreds of MHz) two-tone FM with a lead-salt diode laser was achieved, thus demonstrating the general validity of this technique.

We intend to extend this technique to quantum-cascade lasers, thus making possible to work even in large linewidth regime. Although we encountered some difficulties, as described in the following, we can finally conclude that QC lasers are suitable for this kind of spectroscopy, and we present in this paper the first two-tone molecular spectra ever acquired with a QCL in the mid infrared region.

The complete description of two-tone FM theory is given in detail elsewhere [25]. Here we just recall the main theoretical aspects.

In the most general picture, we have a laser field E_0 at frequency $\nu_0 = \omega_0/2\pi$, and a generic amplitude and angular (frequency and phase) modulation at two different frequencies $\nu_1 = \omega_1/2\pi$ and $\nu_2 = \omega_2/2\pi$ (the 2 "tones"):

$$E_m(t) = E_0(t)\,[1 + M_1 \sin(\omega_1 t + \psi_1)]\,[1 + M_2 \sin(\omega_2 t + \psi_2)] \times \exp\left[i\beta \sin(\omega_1 t) + i\beta \sin(\omega_2 t)\right], \tag{3}$$

where $M_{1,2}$ and $\beta_{1,2}$ are, respectively, the standard AM and FM indices, and $\psi_{1,2}$ the phase differences. A first simplification is suddenly made by posing $M_1 \simeq M_2 = M$, $\beta_1 \simeq \beta_2 = \beta$ and $\psi_1 \simeq \psi_2 = \psi$, since the two modulation frequencies are generally closely spaced and symmetrically generated by mixing a carrier signal of frequency $\nu_m = \omega_m/2\pi$ with a second signal of frequency $\nu_s = \frac{1}{2}\Omega/2\pi$, so that $\omega_1 = \omega_m + \Omega/2$ and $\omega_2 = \omega_m - \Omega/2$, $\Omega \ll \omega_m$.

We are interested on how a generic absorption and dispersion mechanism modifies (3); in other words we are looking for the expression of the resulting beam intensity $I_f(t) = |E_a(t)|^2$, where $E_a(t)$ is the light field after the absorption process.

Calling $\alpha(\omega)$ and $\varphi(\omega)$ the absorption and the phase shift, respectively, introduced by the sample interacting with the laser beam at a frequency ω, we can easily write the expression of the light field after the sample, in the frequency domain:

$$\tilde{E}_a(\omega) = \tilde{E}_m \exp[-\alpha(\omega) - i\varphi(\omega)]\,. \tag{4}$$

Using (3) and (4), it is possible to write the expression for $I_f(t)$ as an infinite sum of rf terms oscillating at frequencies $\omega_{l,k} = l\omega_1 - k\omega_2$, $(l, k \in Z)$. In the two-tone technique, only the slowest component, oscillating at $\omega_{1,1} = \Omega$, is selected

and contributes to the acquired signal:

$$I_{\mathrm{f},\Omega}(t) = I_0(t)\cos(\Omega t)\sum_{n,m=-\infty}^{\infty} r_n r_m r_{n-1}^* r_{m+1}^* e^{-2\alpha(\omega_0+(n+m)\omega_\mathrm{m})} \tag{5}$$

Here r_n are functions of β, M and ψ:

$$r_n(\beta, M, \psi) = J_n(\beta) + \frac{M}{2\mathrm{i}}\left[J_{n-1}(\beta)e^{\mathrm{i}\psi} - J_{n+1}(\beta)e^{-\mathrm{i}\psi}\right]. \tag{6}$$

Some important conclusions can be inferred from (5). First of all, we see that the amplitude of the two-tone signal is proportional to the intensity of the incident beam $|E_0|^2$; the frequency dependance is given by the infinite sum of absorption-like terms. Its effect is to replicate the absorption profile $\alpha(\omega)$, with different amplitudes, starting from $\omega = \omega_0$ and with a constant frequency spacing $\Delta\omega = \pm\omega_\mathrm{m}$. If this spacing is larger than the characteristic width of the absorption line the "comb" structure is perfectly resolved, otherwise the final profile results from a mixing of adjacent components.

The number of non-negligible side peaks of the two-tone signal, as we have already noticed, depends on the r_n parameters, and consequently on the β, M and ψ values. By numerical calculations in a wide range of parameter values [25], it is possible to extract the following simple but useful rules.

For pure frequency modulation ($M = 0$) the signal profile is always symmetric with respect to ω_0, and the number of relevant side peaks is proportional to β.

On the other hand, any pure amplitude modulation ($\beta = 0$) is represented by only three peaks: the optical carrier and two sidebands, all the three with the same sign. This explains why a simultaneous presence of FM and AM determines, with respect to a pure FM signal, an asymmetry between left and right sidebands, which becomes evident for $M > 0.01\beta$.

In conclusion, even a very qualitative examination of the two-tone signal can give information on the real mixing of FM and AM processes on the laser. We will refer to these topics later, when we will examine the experimental results.

We have not yet mentioned the key point of the two-tone technique, especially with respect to standard FM. As we have seen, only the frequency ω_m is involved in determining the resulting signal profile: it is actually the relevant frequency for spectroscopic detection. But the signal itself is modulated at frequency Ω. As we have seen, Ω can be several orders of magnitude smaller than ω_m. It depends on how close the two initial frequencies ω_1 and ω_2 are chosen. In this way, the information contained into the high frequency modulated two-tone signal is transferred to very low frequencies, and can be detected by low-noise, narrow-band detectors. The two-tone, thus, provides a double improvement to the intrinsic noise performances: the benefit coming from the high-frequency modulation lies in shifting the signal to regions where the noise of the laser source is reduced, while the low-frequency acquisition reduces the detection bandwidth and allows one to choose the best detection condition.

3 Experimental set-up

In our experimental set-up two different Fabry–Pérot type cw-emitting QC lasers have been used: one at 8.06 μm wavelength for FM spectroscopy on N_2O, and one at 7.3 μm wavelength for 2T spectroscopy on CH_4. Their working conditions are similar: typical temperature and threshold

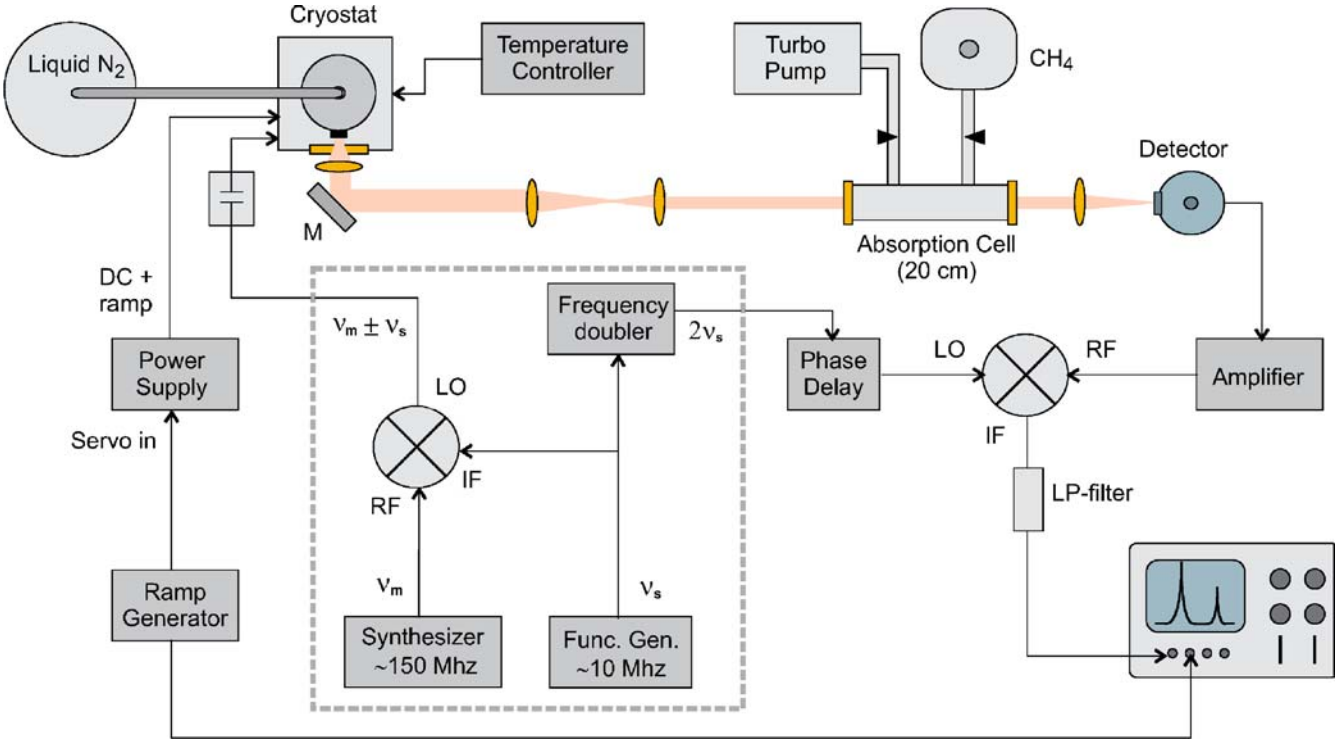

FIGURE 1 Schematic drawing of the experimental set-up. FM and 2T techniques only differ in the generation of the modulating signal (in the *dashed box* we have reported the more complex 2T arrangement)

current are about 80 K and 450 mA, respectively, and the emitting power is up to 40 mW. A liquid N_2 cryostat is used in order to stabilize, within about 10 mK, the laser.

Both lasers have shown a considerable degradation of their behavior during the experimental activity, due to the repeated thermal cycles, the high current flows and, above all, to the direct application on the laser of the modulation signals, without any filtering. In particular, we have noticed an increase of the threshold current and a worsening of their spectral purity. For this reason, after the first FM spectroscopy tests, we have replaced the 8.06 μm wavelength device with the other working at 7.3 μm.

The strongly diverging beam is transmitted by a ZnSe AR-coated window and collimated by a short focal length paraboloidal reflector, then substituted by a germanium lens collimator. After adjusting the beam dimensions by a telescope, we directed the laser radiation to a 20-cm long cell, filled with the sample gas. Radiation is then collected by a fast Hg-Cd-Te photodetector (Kolmar Technologies, 170 MHz bandwidth).

The dc current supply is provided by a homemade low-noise regulated current generator, which includes the possibility of current ramping for frequency sweeping around the spectral feature.

The wavelength tunability vs. temperature and current is about 2 GHz/K and 100 MHz/mA respectively (over a frequency interval of about 1 cm^{-1}) for both lasers.

In Fig. 1, the set-up for 2T spectroscopy is shown. It is the same as the one used for FM spectroscopy, the only difference being in the processing of the modulation signal.

3.1 *Noise and frequency response analysis*

By measuring the voltage vs. current response of the device above threshold we obtain a dynamic impedance of less than 1 Ω (about 0.65 Ω): this may be a serious problem in coupling the rf signal to the laser.

As a first solution we decided to adopt the simplest configuration, in order to test the behavior of the laser in a very basic set-up. We have, thus, assembled a bias-T circuitry, consisting of a dc line equipped with an inductance in order to reject the backward rf modulation and an rf input uncoupled from the dc line by a capacitor. Both the inductance and the capacitor are external to the cryostat, just before the feed-trough connections. The dc and rf lines run independently inside the cryostat and join directly on the laser cathode. Since the dynamic impedance of the QC laser above threshold is very low, we need to match the rf modulation line by adding a low-temperature SMD-type 50 Ω resistor in series with the capacitor. It is inserted inside the cryostat, very close to the laser (about 1 cm). In this way the 50 Ω line carrying the modulating signal is expected to be matched with the correct load when the laser is working.

In a first test, the rf coupling efficiency was characterized as a function of the frequency, by measuring the power directly reflected through the bias-tee. A directional coupler was inserted in the rf line, in order to monitor the total input rf power (P_I) and the reflected component of a pure modulation note generated by a synthesizer and sent to the QCL (P_R). These data were then compared with measurements taken after replacing the QC laser with a 50 Ω termination. Results are shown in Fig. 2a. The input power dependance on frequency reflects the behavior observed with the perfectly matched load, though very large oscillations around the expected curve are measured. The same effect is revealed also when monitoring the reflected signal. However, in some regions of the analyzed spectrum (0–700 MHz), some other effects appear and cause stronger negative peaks on the reflected signal, without affecting in a sensible way the input signal power. In these regions the signal coupling is expected to get better. By normalizing the curve of the reflected signal power with the input signal power curve, the short period oscillations disappear and the peaks where best coupling takes place become more evident. Figure 2b shows the transmission coefficient $T = 1 - P_R/P_I$ obtained from the acquired curves. The transmission drops with frequency quite rapidly, but it is possible to recognize the sharp positive peaks that likely correspond to a better coupling of the rf signal.

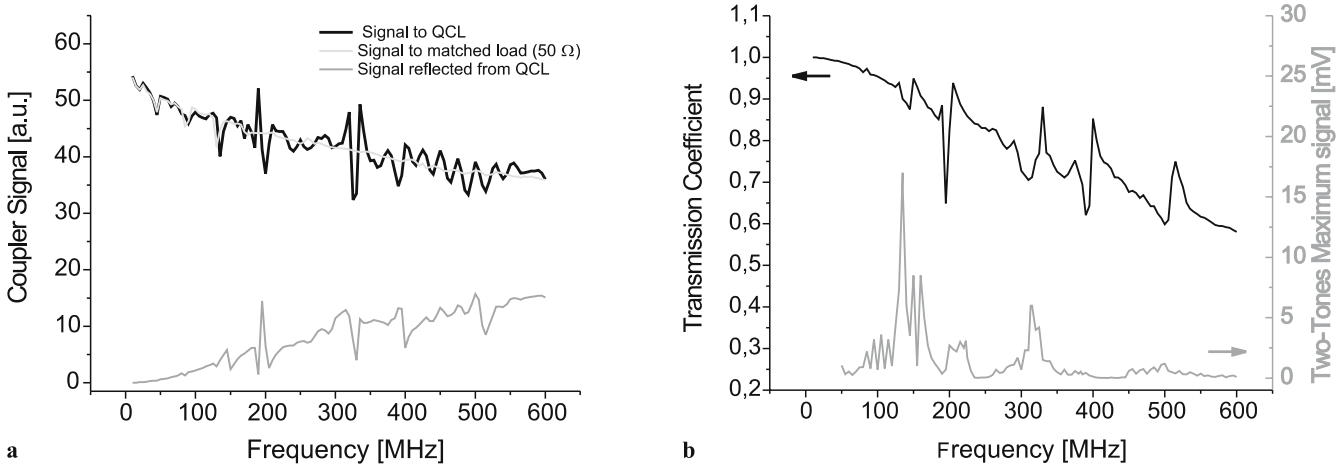

FIGURE 2 (**a**) Dependance of the input and reflected power of the rf signal on frequency. The overall behavior of the input power follows the expected trend obtained by replacing the laser with a 50Ω matched load; (**b**) from the measurements above we obtained the transmission coefficient T of our system. The peaks point out the frequencies at which best signal coupling takes place. This is indeed verified by directly measuring the amplitude of the two-tone signal acquired in presence of a molecular line, here shown in *gray* (see Sect. 4.2)

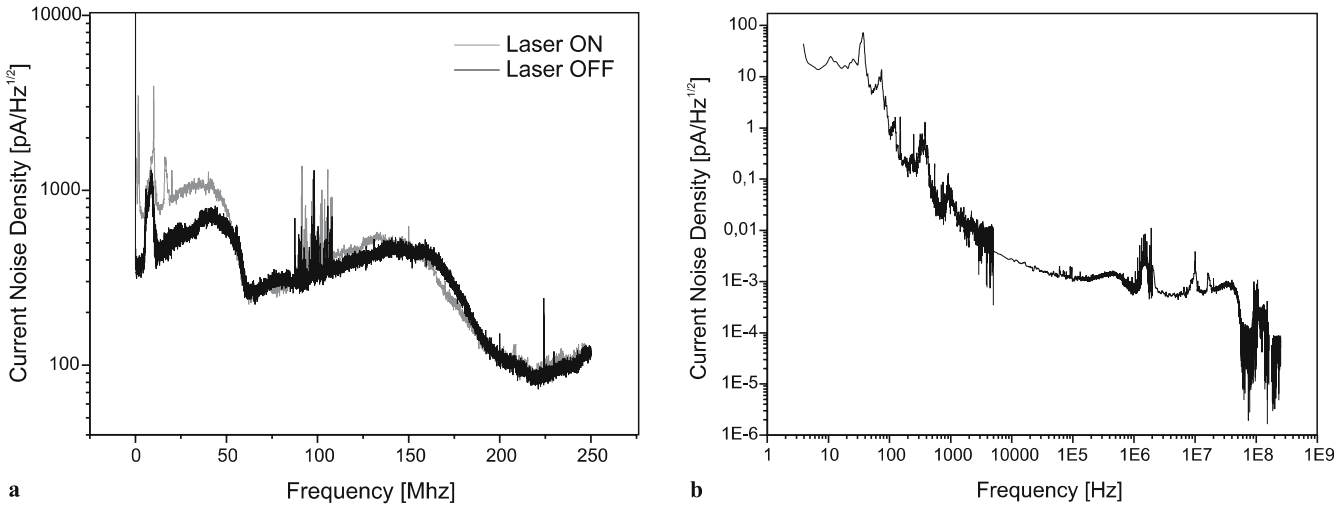

FIGURE 3 (**a**) Comparison between the noise spectral density from the detector with and without the laser light; (**b**) laser source noise spectral density after subtraction of the detector dark noise

The results presented above allow one to reach some important conclusions. First of all the simple impedance matching technique that we have adopted can work, but only for few discrete ν_m values. If one is interested in a more homogeneous frequency response or in modulation frequencies higher than a few hundred MHz, more careful matching has to be done, for example by inserting an impedance transformer in the rf line. For this reason we are building a compact passive rf matching network, composed by a broadband bias-tee followed by an impedance transformer and suitable to be inserted into the cryostat and to work at low temperatures. Preliminary tests show encouraging performances.

A second important test has been done on the noise spectral density of both the detector and the laser sources. Figure 3a shows a direct comparison of the two noise profiles in the whole detector bandwidth. By subtracting these quantities, we obtain the laser noise density exceeding out from the detector background, plotted in Fig. 3b in a log-log scale, in order to zoom out the very-low frequencies contributions.

We can make two important considerations:

– For what concerns the FM spectroscopy, we can notice that the detector bandwidth is of the order of the Doppler broadening of our lines. An optimal FM configuration would have required larger modulation frequencies and thus faster detectors.
– The source contribution to the total noise is located mainly in the very low frequency region (below a few hundreds of Hz), while the remaining contribution is of the same order of the detector noise. Since the former is cut also in direct absorption by means of the 1 kHz frequency sweeping ramp, it does not contribute to the improvement of the S/N ratio. For this reason the actual improvement due to the laser noise reduction is expected to be small.

4 Spectroscopic results

4.1 FM

From the analysis of the laser power spectral density at the detector, the modulation frequency was set at values ranging from 150 to 170 MHz, with a chosen sidebands level of a few dBm. The modulation depth can be estimated within a few-percent (1–2 %) by measuring the sideband vs. carrier amplitude level with the analyzer [26].

In this configuration, the detector output signal was amplified by a low-noise amplifier and demodulated by a double-balanced mixer. The demodulation process yields a voltage output which, in the proximity of a line center, is proportional to any amplitude or phase difference between the carrier-to-sideband beat signals, eventually caused by interaction of infrared radiation with the gas sample. Proper phase adjustment between the detector signal and the mixer local oscillator was carried out by a variable time delay in order to extract only the in-phase or the quadrature component of the detected signal.

In Fig. 4 we show several lines of N_2O molecule, recorded with the described FM scheme, with a gas pressure of 500 mTorr in the cell.

What we can notice is the very good signal-to-noise ratio of the recorded spectrum (2500 for the strongest line). The fig-

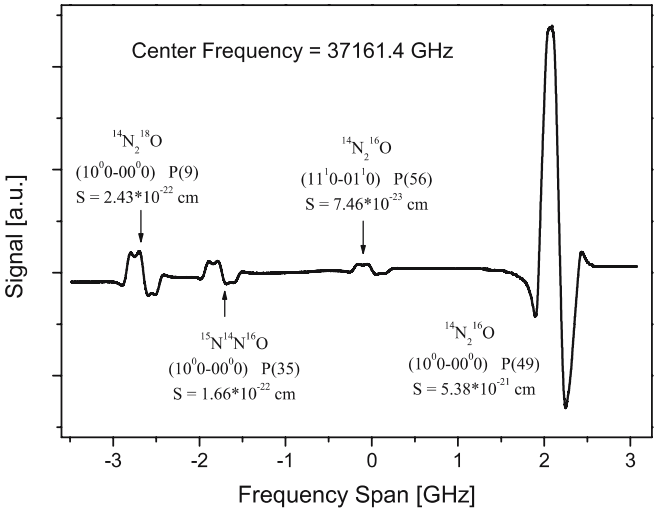

FIGURE 4 FM recorded spectra of some N_2O molecular transitions. Laser temperature and current are $T = 81.2$ K, $I = 565$–610 mA; gas pressure is $P = 500$ mTorr

ure shows the absorption lines of several N_2O isotopomers: the high stability of the signal confirms the QC laser to be a suitable source for isotopic ratio and relative abundance measurements [26]. A comparison with the direct absorption signals (in the same conditions of laser power and gas pressure) shows an improvement in the signal-to-noise ratio of about a factor two. Although this may be a small enhancement, it is what we expected from the reduction of the source noise contribution.

As a last remark, we notice that we are using the detector in its cut off region. This is the reason why a natural implementation is represented by the two-tone technique, since it allows one to keep the same laser modulation frequency while shifting the detected signal to lower frequencies.

4.2 *Two-tone*

In order to generate the two-tone modulating signal, that is the pair of frequencies separated by Ω, we have used a rf mixer driven by a rf synthesizers set to the frequency $\nu_m = \omega_m/2\pi$ and a waveform generator set to the frequency $\nu_s = \frac{1}{2}\Omega/2\pi$. The mixer is used in a "reversed" configuration, with the rf and IF channels as inputs and the LO channel as output. In this way, sideband generation is more efficient, with a very good suppression of the higher order harmonics and the carrier (better than -40 dB). The resulting signal is then amplified and sent to the QCL for the two-tone modulation. After the spectroscopy cell, the laser beam is revealed by the Hg-Cd-Te detector.

We first verified the coupling of the rf signal to the laser by directly observing the detector output signal with a spectrum analyzer, in presence of an absorption line. For this measurement the set parameters are $\Omega = 15$ MHz and ν_m variable from a few MHz to 700 MHz. In correspondence with the absorption peak a signal at a frequency $\nu = 2\pi\Omega$ (the two-tone signal) arises, and we measure its maximum amplitude.

This signal actually appears only for specific ν_m values, showing that coupling of the rf modulation is not constant in the 0–700 MHz range. Comparing the set of frequencies found here with that found before, we see that the two sets almost coincide (Fig. 2).

After this test we have chosen the frequency $\nu_m = 150$ MHz, in order to optimize its coupling to the laser.

The detector signal is then processed for the two-tone measurement: after an amplification stage it is demodulated by means of a second rf mixer, whose local oscillator input frequency $2\nu_s$ is obtained by frequency doubling the signal of the waveform generator (see Fig. 1). After a low-pass filter, the signal is sent to the oscilloscope for the acquisition, with no further amplification stages.

The effective detection bandwidth is fixed by the low-pass filter cut frequency, and in our set-up is 4.8 MHz, eventually rescaled by the number of averaged traces. For a more sensitive detection, a narrower filter should be used.

In Fig. 5a a first comparison between a sequence of lines acquired in direct absorption and with the 2T technique is presented. The gas pressure in the cell is 10 mTorr, resulting in a relative absorption of about 10%. The power level for the modulating signal is about 3 dBm, and $\Omega = 10$ MHz. The frequency sweep is performed by the same 1 ms linear ramp. The profile of the 2T lines is the expected one, supposing the contribution of only the first side peaks. The slight asymmetry in the line profiles is probably caused by the presence of an AM component that, as we have seen in Sect. 2.2, adds opposite contributions on the side peaks and arises from the strong dependance of the laser intensity on the driving current (as indicated by the slope of the direct absorption trace).

This effect is much more evident if ν_m is increased from 150 MHz to 300 MHz. In this situation the line profile becomes that shown in Fig. 5b: The spacing between the central peak (the negative one) and the side peaks increases, and each peak replicates the gaussian lineshape. The left peak, however, is heavily suppressed. In fact, when ν_m increases, the FM modulation index $\beta = \frac{\Delta\nu}{\nu_m}$ decreases, and the relative contribution of the AM gets more important. This is the reason why the asymmetry becomes more evident, as we have noted in Sect. 2.2.

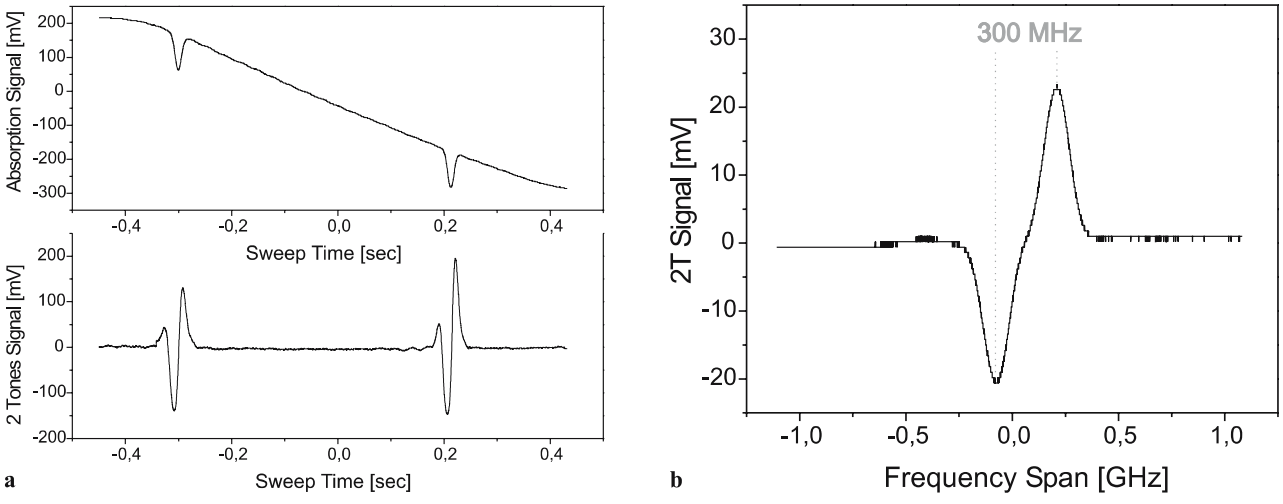

FIGURE 5 (**a**) A comparison is shown between a doublet of CH_4 lines acquired by direct absorption spectroscopy and by 2-tones technique. The improvement on the S/N ratio is about a factor of 4. (**b**) The asymmetry of the line is enhanced if the modulation frequency ν_m is increased (here $\nu_m = 300$ MHz). In this way the modulation index β decreases, and the ratio $\frac{M}{\beta}$ changes from 0.9% to 1.8%, corresponding to the arising of the asymmetry, as reproduced by the simulations in [25]

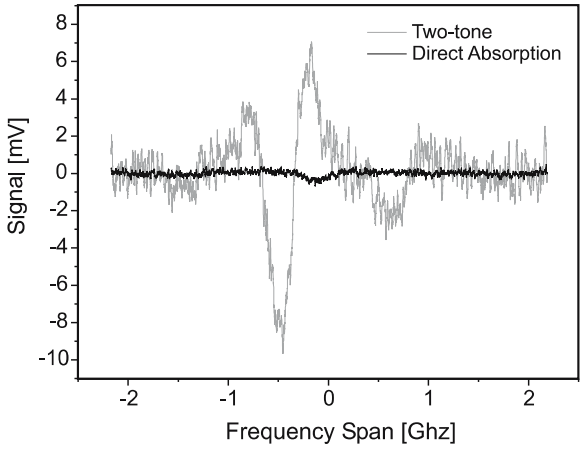

FIGURE 6 The graph shows a measurement performed with a CH_4 pressure in the cell lower than 1 mTorr, leading to a relative absorption of 1%. The S/N ratios for direct absorption and 2-tones spectra are respectively 2.4 and 14. Both traces are the result of a 4-scan averaging (detection bandwidth is consequently rescaled)

Finally we want to show in Fig. 6 the comparison between absorption and two-tone spectroscopy with a very low gas pressure in the cell (less than 1 mTorr). Here the noise becomes more evident in both traces, but the S/N ratio in the two-tone curve is enhanced by a factor of six. This is a significant improvement, which demonstrates the suitability of high frequency modulation techniques on QC lasers. We remark on the fact that, due to the starting very low overall noise level, the enhancement obtained is of the expected order of magnitude.

This enhancement allows one to improve the minimum detectable relative absorption from 4×10^{-3} to 7×10^{-4}. Rescaling by the square root of the effective detection bandwidth (1.2 MHz), we can finally estimate the noise equivalent absorbance to be $6 \times 10^{-7} / \sqrt{(\mathrm{Hz})}$. The sensitivity per unit bandwidth is then enhanced with respect to results already achieved with QC lasers modulated at lower frequencies [27].

4.3 *Conclusions*

In this paper we have presented what we believe to be the first thorough application of high-frequency modulation spectroscopic techniques to QC lasers. Both for FM and 2T, the signal profile is the expected one, according to our experimental conditions. The maximum measured enhancement of the S/N ratio with respect to the direct absorption results is about six times. Such an improvement is of the expected order of magnitude, considering both the detector response features and the very low noise floor of our laser source. This paves the way to applications of QC lasers to high sensitivity monitoring of even broad molecular lines in real atmospheric pressure environments, the remaining obstacle being efficient coupling to the laser of GHz frequency modulation.

ACKNOWLEDGEMENTS The authors want to thank Dr. Giovanni Giusfredi for useful discussions and suggestions and Dr. Jacopo Catani and Dr. Iacopo Galli for their contribution to this work. This work has been partly funded by Italian FIRB Project RBNE01KZ94.

REFERENCES

1 T.F. Gallagher, R. Kachru, F. Gounand, G.C. Bjorklund, W. Lenth, Opt. Lett. **7**, 28 (1982)
2 J. Faist, F. Capasso, D.L. Sivco, C. Sirtori, A.L. Hutchinson, A.Y. Cho, Science **264**, 553 (1994)
3 C. Sirtori, J. Faist, F. Capasso, D.L. Sivco, A.L. Hutchinson, A.Y. Cho, IEEE Photon. Technol. Lett. **9**, 294 (1997)
4 D. Hofstetter, M. Beck, T. Aellen, J. Faist, U. Oesterle, M. Ilegems, E. Gini, H. Melchio, Appl. Phys. Lett. **78**, 1964 (2001)
5 S. Blaser, D.A. Yarekha, L. Hvozdara, Y. Bonetti, A. Muller, M. Giovannini, J. Faist, Appl. Phys. Lett. **86**, 041 109 (2005)
6 F. Capasso, C. Gmachl, R. Paiella, A. Tredicucci, A.L. Hutchinson, D.L. Sivco, J.N. Baillargeon, A.Y. Cho, H.C. Liu, IEEE J. Quantum Electron. **QE-6**, 931 (2000)
7 C. Gmachl, F. Capasso, A. Tredicucci, D.L. Sivco, J.N. Baillargeon, A.L. Hutchinson, A.Y. Cho, Mater. Sci. Eng. B **75**, 93 (2000)
8 J. Faist, F. Capasso, D.L. Sivco, A.L. Hutchinson, C. Sirtori, S.N.G. Chu, A.Y. Cho, Appl. Phys. Lett. **65**, 2901 (1994)
9 A.A. Kosterev, F.K. Tittel, C. Gmachl, F. Capasso, D.L. Sivco, J.N. Baillargeon, A.H. Hutchinson, A.Y. Cho, Appl. Opt. **39**, 6866 (2000)
10 G. Gagliardi, F. Tamassia, P. De Natale, C. Gmachl, F. Capasso, D.L. Sivco, J.N. Baillargeon, A.L. Hutchinson, A.Y. Cho, Eur. Phys. J. D **19**, 327 (2002)
11 R.M. Williams, J.F. Kelly, J.S. Hartman, S.W. Sharpe, M.S. Taubman, J.L. Hall, F. Capasso, C. Gmachl, D.L. Sivco, J.N. Baillargeon, A.Y. Cho, Opt. Lett. **24**, 1844 (1999)
12 M.S. Taubman, T.L. Myers, B.D. Cannon, R.M. Williams, F. Capasso, C. Gmachl, D.L. Sivco, A.Y. Cho, Opt. Lett. **27**, 2164 (2002)
13 G. Wysocki, R.F. Curl, F.K. Tittel, R. Maulini, J.M. Bulliard, J. Faist, Appl. Phys. B **81**, 769 (2005)
14 J.T. Remillard, D. Uy, W.H. Weber, F. Capasso, C. Gmachl, A.L. Hutchinson, D.L. Sivco, J.N. Baillargeon, A.Y. Cho, Opt. Express **7**, 243 (2000)
15 G. Duxbury, N. Langford, M.T. McCulloch, S. Wright, Chem. Soc. Rev. **34**, 921 (2005)
16 L.S. Ma, J. Ye, P. Dube, J.L. Hall, J. Opt. Soc. Am. B **12**, 2255 (1999)
17 D.S. Bomse, A.C. Stanton, J.A. Silver, Appl. Opt. **31**, 718 (1992)
18 F.S. Pavone, M. Inguscio, Appl. Phys. B **56**, 118 (1993)
19 G.C. Bjorklund, Opt. Lett. **5**, 15 (1980)
20 G.C. Bjorklund, M.D. Levenson, W. Lenth, C. Ortiz, Appl. Phys. B **32**, 145 (1983)
21 H.E. Warner, W.T. Conner, R.C. Wood, J. Chem. Phys. **81**, 5413 (1984)
22 C.S. Gudeman, M.H. Begemann, J. Pfaff, R.J. Saykally, Opt. Lett. **8**, 310 (1983)
23 D.T. Cassidy, J. Reid, Appl. Phys. B **29**, 279 (1982)
24 G.R. Janik, C.B. Carlisle, T.F. Gallagher, J. Opt. Soc. Am. B **3**, 1070 (1986)
25 D.E. Cooper, R.E. Warren, J. Opt. Soc. Am. B **4**, 470 (1987)
26 G. Gagliardi, S. Borri, F. Tamassia, F. Capasso, C. Gmachl, D.L. Sivco, J.N. Baillargeon, A.L. Hutchinson, A.Y. Cho, Isotopes Environ. Health Stud. **41**, 313 (2005)
27 K. Namjou, S. Cai, E.A. Whittaker, J. Faist, C. Gmachl, F. Capasso, D.L. Sivco, A.Y. Cho, Opt. Lett. **23**, 219 (1998)